sustainability

MDPI

Article

Influence of Deicer on Water Stability of Asphalt Mixture under Freeze–Thaw Cycle

Mingjun Guo [1], Viktor Pavlovich Kovalskiy [1], Tengfei Nian [2,*] and Ping Li [2]

[1] Faculty of Civil Engineering, Thermal Power Engineering and Gas Supply, Vinnytsia National Technical University, Voiniv-Internatsionalistiv St. 7, 21000 Vinnytsia, Ukraine
[2] School of Civil Engineering, Lanzhou University of Technology, Lanzhou 730050, China
* Correspondence: tengfeinian@lut.edu.cn

Abstract: In seasonal frozen soil areas, the repeated freeze–thaw cycle of internal moisture in asphalt mixture in winter and spring will accelerate the peeling of asphalt film and aggravate the water damage of asphalt pavement. It is of great significance to carry out the attenuation law of mechanical properties of asphalt mixture under freeze–thaw cycles to prevent and reduce the economic losses caused by water damage to asphalt pavement. This study will investigate the impact of deicer application on the water stability of asphalt mixtures within the climatic conditions prevalent in Northwest China. Specifically, freeze–thaw cycle tests were administered to two types of dense-graded asphalt mixtures under three distinct deicer solutions and three disparate low-temperature environments. The Marshall water immersion test and freeze–thaw splitting test were employed to evaluate the water stability of asphalt mixtures subject to multiple factors, and the relative importance of each factor was statistically analyzed using the acquired data. Results demonstrated that AC-13 and AC-16 asphalt mixtures (AC is asphalt-concrete, which is asphalt concrete, and 13 or 16 represents the maximum particle size of aggregate (13 mm or 16 mm)), saturated in 15% CH_4N_2O, 20% NaCl, and 20% CH_2CH_3OH solutions, underwent a varying number of freezing–thawing cycles (0, 5, 10, 15, 20, 25, and 30) at temperatures of −5 °C, −15 °C, and −25 °C, respectively, displayed a discernible decline in their residual stability MS_0 and freeze–thaw splitting tensile strength ratio TSR. This decline was particularly marked when temperatures dropped below the solution's freezing point. Disregarding the fixed factors of weather variation (different low-temperature environments) and road service duration (number of freezing–thawing cycles), the aggregate grading imposed a more pronounced influence on asphalt mixture water stability than the presence of deicers.

Keywords: road engineering; asphalt mixture; freeze–thaw cycle; water stability; deicer

check for updates

Citation: Guo, M.; Kovalskiy, V.P.; Nian, T.; Li, P. Influence of Deicer on Water Stability of Asphalt Mixture under Freeze–Thaw Cycle. *Sustainability* **2023**, *15*, 13707. https://doi.org/10.3390/su151813707

Academic Editor: Ramadhansyah Putra Jaya

Received: 31 July 2023
Revised: 10 September 2023
Accepted: 13 September 2023
Published: 14 September 2023

Copyright: © 2023 by the authors. Licensee MDPI, Basel, Switzerland. This article is an open access article distributed under the terms and conditions of the Creative Commons Attribution (CC BY) license (https://creativecommons.org/licenses/by/4.0/).

1. Introduction

Asphalt pavement, celebrated for its low vibrational attributes, minimal noise levels, and ease of maintenance, is extensively adopted in the construction of high-grade highways [1]. However, in winter months, the presence of ice or snow can significantly reduce the skid resistance of asphalt surfaces, consequentially escalating the frequency of traffic accidents and the potential for casualties [2,3]. Currently, to ensure vehicular safety, highway maintenance departments predominantly employ chemical, mechanical, and heating methods to eradicate road ice and snow. The long-standing preferred technique has been deicer distribution, attributable to its high efficacy, cost-effectiveness, and simplicity of operation. Foreseeably, this approach will remain dominant in the near term, as alternatives are not expected to supplant it [4]. Despite its benefits, the widespread application of deicers poses environmental challenges to the surrounding road areas and inflicts considerable damage to the pavement [5–7].

Upon the dispersion of deicer on roadways, its solution permeates both the pavement and the surrounding environment. Prior to considerable precipitation-induced dilution,

the pavement remains enveloped in an environment with a high concentration of the deicer solution [8,9]. This effect is particularly pronounced in areas like Northwest China, characterized by limited rainfall. Though numerous studies have focused on the impact and mechanisms of deicers on cement concrete [10–13], investigations into their effects on asphalt concrete are comparatively scarce due largely to its complex viscoelastic nature, as opposed to the simpler elastic–plastic behavior of cement concrete [14–17]. Setiadji [18] subjected asphalt mixtures to wet–dry cycles in varied concentrations of chloride solutions, concluding that chloride may predominantly contribute to asphalt mixture damage. Similarly, Xiong [19] suggested that crystallization erosion, instigated by salt solution seeping into the voids and cracks of the asphalt mixture, is a vital factor in asphalt mixture deterioration. Consequently, deicers lingering in the roadside environment could potentially induce significant harm to the asphalt mixture.

During frigid winters, substantial temperature disparities instigated by daily fluctuations or weather conditions can induce multiple freeze–thaw cycles of the deicer solution [20,21]. The salt solution infiltrating the exterior voids of the mixture can generate frost heave forces upon freezing [22], prompting the voids within the mixture to evolve into interconnected open gaps, thereby hastening asphalt mixture degradation. Amini's research [23] into the impact of salt solution on asphalt mixture deterioration under freeze–thaw cycles demonstrated that the joint action of water and deicer amplifies asphalt mixture deterioration; furthermore, it was found that asphalt mixtures with a higher proportion of fine aggregates exhibit enhanced erosion resistance. Through freeze–thaw cycle testing, Feng [24] established that salt significantly affects the low-temperature performance of asphalt mixtures. It was discerned that when salt content is below 3%, freeze–thaw cycles primarily impact the asphalt mixture's low-temperature performance; however, when salt content exceeds 3%, salt erosion accelerates asphalt mixture degradation. According to Guo et al. [25], the bonding interface between asphalt and aggregate under salt immersion and freeze–thaw cycles deteriorates faster than under pure water conditions. Wang's in-depth analysis [26], employing semi-circular bending tests, studied the effects of asphalt type, freeze–thaw cycle frequency, and deicer concentration on asphalt mixture crack resistance, indicating a gradual decrease in crack resistance with an increase in freeze–thaw cycle frequency and salt concentration. Huang Xinyan et al. [27] found that the likelihood of asphalt film detachment increases in the presence of salt. Zhang's [28] research on the application of microwave heating technology in repairing microcracks resulting from freeze–thaw cycle damage, conducted on two different asphalt mixtures, suggested that freeze–thaw damage and microwave heating alter the material's internal pore structure. As such, they proposed optimal healing times and depths for the two mixtures, offering novel insights into the damage from freeze–thaw cycles and the mechanism of microwave healing.

Current research predominantly focuses on the impact of deicers on the low-temperature stability of asphalt concrete, with scant attention paid to water stability. The majority of these studies emphasize single-factor alterations, resulting in a deficit of comprehensive evaluations of the multi-factor influence of deicers on the water stability of asphalt mixtures. Water stability embodies the competency of asphalt blends to preserve their physico-mechanical properties amidst water exposure. This metric provides an essential gauge for evaluating the capacity of asphalt mixtures to sustain their structural integrity, preclude material detachment, and conserve compressive and shear strength under hydric conditions, for instance, precipitation and groundwater intrusion. Water is the primary agent inducing various forms of early damage to asphalt pavements. The presence of water alters the physical and chemical properties of the asphalt binder, diminishes the adhesion between asphalt and aggregate, and, under the effect of other factors, instigates a range of pavement diseases, impacting both service performance and lifespan [29,30]. Consequently, it is crucial to investigate the changes in water stability of asphalt concrete after exposure to deicer erosion and freeze–thaw cycles and to identify the main factors contributing to water stability damage under multiple influences.

In the initial phase, the research team established nine monitoring points on high-grade highways in Gansu Province, China. Wind velocity and direction, precipitation,

solar radiation intensity, and atmospheric humidity were procured via the CaipoBase compact weather station, whereas asphalt pavement temperatures were gauged using soil temperature sensors placed at depths of 10 cm, 20 cm, 30 cm, 40 cm, and 50 cm. These measurements were conducted on an hourly basis, revealing that the minimum internal temperature of the road infrastructure could descend to −15 °C [21]. Concurrently, the freezing point of various deicers was assessed in the laboratory, yielding data on the freezing points of different concentrations of commonly used deicers [20,21]. Building upon these findings and taking into account the unique climatic and hydrological characteristics of Northwest China [16,31], this study selected three suitable deicer solutions for freeze–thaw cycle testing on two types of graded asphalt mixtures under three low-temperature conditions. The water stability of the asphalt concrete was examined via the Marshall water immersion test and the freeze–thaw splitting test. A statistical analysis was conducted to identify the primary factor affecting the water stability of asphalt mixtures due to deicer to prevent and reduce the economic losses caused by water damage to asphalt pavement.

2. Selection of Raw Materials

2.1. Asphalt

This present study employs KL-90 petroleum asphalt sourced from the Xinjiang Karamay refinery. Key technical parameters were ascertained in accordance with the "Standard Test Methods for Bitumen and Bituminous Mixtures for Highway Engineering" (JTG E20–2011) [32], all of which adhered to the stipulations of the "Technical Specification for Construction of Highway Asphalt Pavements" (JTG F40–2017) [33]. The technical parameters of the asphalt are presented in Table 1.

Table 1. Technical indexes of asphalt.

Index	Test Result	Requirement	Test Method
Penetration (25 °C, 100 g, 5 s)/0.1 mm	88	80~100	T0604
Penetration Index	−1.1	−1.5~+1.0	T0604
Extensibility (15 °C)/cm	>100	≥100	T0605
Softening Point/°C	48	≥45	T0606
Flash Point/°C	300	≥245	T0611
Density (15 °C)/(g·cm^{-3})	1.033	Measured value	T0603

2.2. Aggregate

The selected coarse aggregate, fine aggregate, and mineral powder are all derived from the diabase sourced from Wangjiaping Material Yard in Lanzhou City, Gansu Province. The pertinent technical parameters were examined in accordance with the "Test Methods of Aggregate for Highway Engineering" (JTG E42–2005) [34] and were found to satisfy the technical stipulations outlined in the "Technical Specification for Construction of Highway Asphalt Pavements" (JTG F40–2017) [33], as depicted in Tables 2–4.

Table 2. Technical indexes of coarse aggregate.

Index	Test Result	Requirement	Test Method
Crushed Stone Value/%	17.9	≤28	T0316
Los Angeles Abrasion Loss/%	17.2	≤30	T0317
Apparent Particle Density	2.81	≥2.5	T0304
Solmdness/%	10.9	≤12	T0314
Water Absorption/%	1.5	≤3	T0304

Table 3. Technical indexes of fine aggregate.

Index	Test Result	Requirement	Test Method
Apparent Particle Density	2.73	≥2.50	T0328
Solmdness/%	9.1	≤12	T0340
Mud Content/%	2.0	≤3	T0333
Sand Equivalent/%	76	≥60	T0334

Table 4. Technical indexes of mineral powder.

Index	Test Result	Requirement
Density/(t·m^{-3})	2.82	≥2.5
Water Absorption/%	0.89	≤1
Hydrophilic Coefficient/%	≤1	≤1

2.3. Deicer

To investigate the impact of varying deicers on the performance of asphalt mixtures, urea, industrial salt, and ethanol were identified as subjects of this study. Owing to their widespread use in snow-melting and deicing operations on winter roads worldwide, the findings of this research can offer an authentic depiction of the actual scenario. Industrial salt, or sodium chloride, is extensively employed for ice and snow-melting on winter roads, attributed to its pronounced snowmelt capacity and cost-effectiveness. Urea, a quintessential non-salt organic compound, has applications extending beyond agriculture to function as a snow-melting and deicing agent for winter roads. Despite urea's freezing point reduction effect being lesser than that of sodium chloride, its comparatively lower environmental footprint and non-corrosive properties make it a favored choice in regions prioritizing environmental protection. Representing alcohol-based deicers, ethanol, with its lower freezing point and volatility, can be employed to simulate harsher winter conditions in experimental setups. Urea (CH_4N_2O) produced by Gansu Liuhua (Group) Co., Ltd., Lanzhou, China, industrial salt (NaCl) by Golmud Baojin Chemical Trading Co., Ltd., Geermu, China, and absolute ethanol (CH_2CH_3OH) by Tianjin Beichen Fangzheng Reagent Factory, Tianjin, China, were selected as the three types of deicers. Their technical indices conform to relevant stipulations. The associated physical properties are outlined in Tables 5–7.

Table 5. Technical indexes of urea (CH_4N_2O).

Mass Fraction of Total Nitrogen (N)/%	Mass Fraction of Biuret/%	Water/%	Mass Fraction of Iron (in Fe)/%	Alkalinity (in the Mass Fraction of NH_3)/%	Mass Fraction of Sulfate (in SO_4^{2-})/%	Mass Fraction of Water Insoluble Substance/%
≥46.4	≤0.5	≤0.3	≤0.0005	≤0.01	≤0.005	≤0.005

Table 6. Technical indexes of industrial salt (NaCl).

NaCl/(g/100 g)	Water/(g/100 g)	Insoluble Matter/(g/100 g)	Total Calcium and Magnesium Ions/(g/100 g)	Sulfate Ion/(g/100 g)
≥99.1	≤0.30	≤0.05	≤0.25	≤0.30

2.4. Design of Mix Proportion

This study employed two variants of asphalt mixtures, AC-13 and AC-16, with their respective maximum granular sizes being 13.2 mm and 16 mm. The compositions of the mineral aggregate gradation are presented in Figures 1 and 2. The optimal asphalt

aggregate ratios were established through the Marshall compaction test at 5.1% for AC-13 and 4.5% for AC-16. The theoretical maximum densities were determined to be 2469 kg/m^3 for AC-13 and 2570 kg/m^3 for AC-16.

Table 7. Technical indexes of absolute ethanol (CH_2CH_3OH).

Mass Fraction of Ethanol (CH_2CH_3OH)/%	Density (20 °C)/(g/mL)	Mixing Test with Water	Mass Fraction of Evaporation Residue/%	Mass Fraction of Water/%	Mass Fraction of Methanol/%	Mass Fraction of Isopropanol/%
≥99.7	0.789–0.791	Qualified	≤0.001	≤0.3	≤0.05	≤0.01

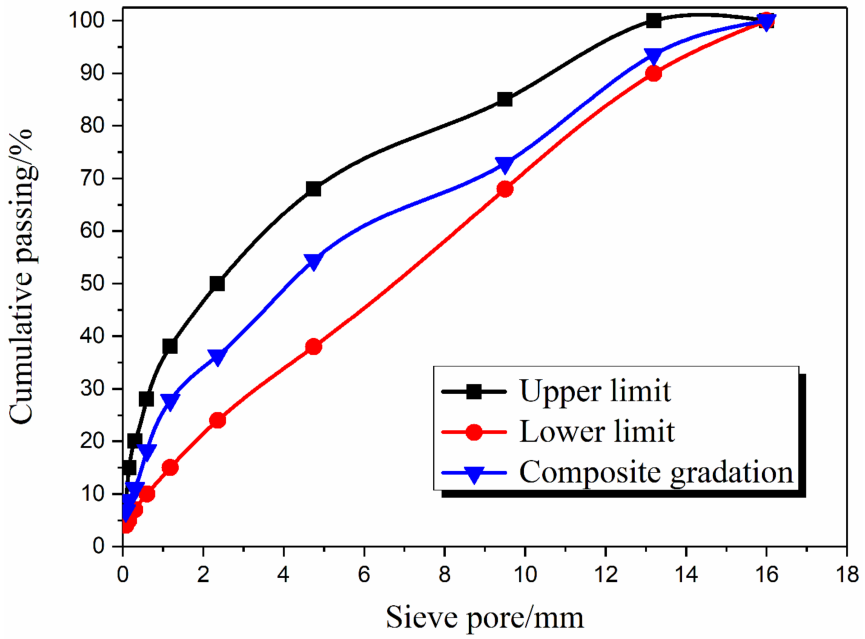


Figure 1. Synthetic grading curve of AC-13.

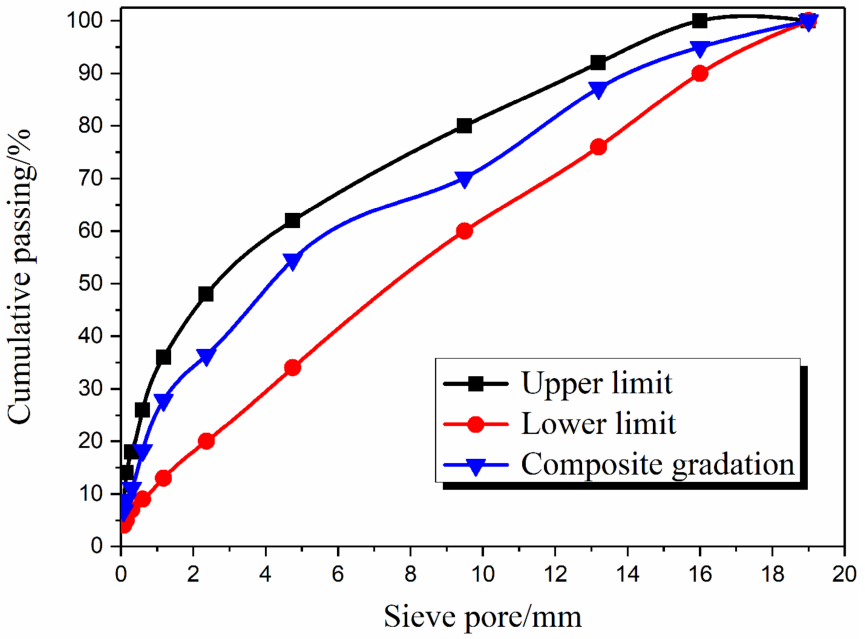


Figure 2. Synthetic grading curve of AC-16.

3. Test Methods

3.1. Test Method for Freeze–Thaw Cycles

Three deicers (urea, sodium chloride, and absolute ethanol) were employed in this study. Given their effectiveness in snow melting and the specific climatic and hydrological conditions of Northwest China, 15% urea (15% CH_4N_2O), 20% industrial salt (20% NaCl), and 20% absolute ethanol (20% CH_2CH_3OH) solutions were prepared for freeze–thaw cycling. Marshall specimens of AC-13 and AC-16 were prepared to undergo 0, 5, 10, 15, 20, 25, and 30 freeze–thaw cycles at temperatures of −5 °C, −15 °C, and −25 °C. It is crucial to note that these cycles were performed separately for each of the deicer solutions and at each of the three temperatures, making for a comprehensive range of testing conditions. At the cycle's commencement, specimens were submerged in the deicer solutions for 12 ± 0.5 h, as depicted in Figure 3. Post-immersion, specimens were transferred to a temperature control chamber for 12 ± 0.5 h, with the chamber's temperature discrepancy being less than 1 °C, as illustrated in Figure 4. After the freezing phase, specimens were removed and reimmersed in the deicer solutions for the subsequent cycle. Given the volatility of absolute ethanol, its solution was remade after each cycle, while urea and industrial salt solutions were prepared once every three cycles. Post freeze–thaw cycles, the Marshall specimens underwent Marshall water immersion tests and freeze–thaw splitting tests in accordance with the "Standard Test Methods for Bitumen and Bituminous Mixtures for Highway Engineering" (JTG E20-2011) [32].



Figure 3. Test specimens immersed in deicer solutions.

3.2. Marshall Water Immersion Test

Marshall specimens were fabricated in adherence to the T0702-2011 test methodology delineated in the "Standard Test Methods for Bitumen and Bituminous Mixtures for Highway Engineering" (JTG E20-2011) [32]. The specimens, with diameters and heights of 101.6 ± 0.2 mm and 63.5 ± 1.3 mm, respectively, were compacted 75 times on both sides. Following fabrication, these cured specimens were subjected to freeze–thaw cycles in three distinct deicer solutions at three varying temperatures as per the outlined test procedure. Post freeze–thaw cycling, the Marshall water immersion test was implemented, conforming to the T0709-2011 test procedure in the "Standard Test Methods for Bitumen

and Bituminous Mixtures for Highway Engineering" (JTG E20-2011) [32]. The specific steps of the testing procedure involved partitioning eight completed freeze–thaw cycle Marshall specimens into two sets, each containing four specimens. The first quartet of specimens was positioned in a constant temperature water bath for a duration of 30 min, while the second quartet was subjected to the same conditions for 48 h. Upon completion of the respective insulation times, the specimens were promptly retrieved and placed on a Marshall stability tester for evaluation. After concluding the test, the residual stability was computed using Formula (1), and an average value was obtained. The test was facilitated using the Marshall stability tester (SYD-0709A-1), supplied by Shanghai Changji Geological Instrument Co., Ltd., Shanghai, China, with the loading speed kept within the range of 50 ± 5 mm/min. The constant temperature water bath was maintained at 60 ± 1 °C.

$$MS_0 = \frac{MS_1}{MS} \times 100 \quad (1)$$

where:

MS_0 is residual stability of test specimen (%);
MS_1 is stability of test specimen after 48 h of immersion in water (kN);
MS is stability of test specimen (kN).

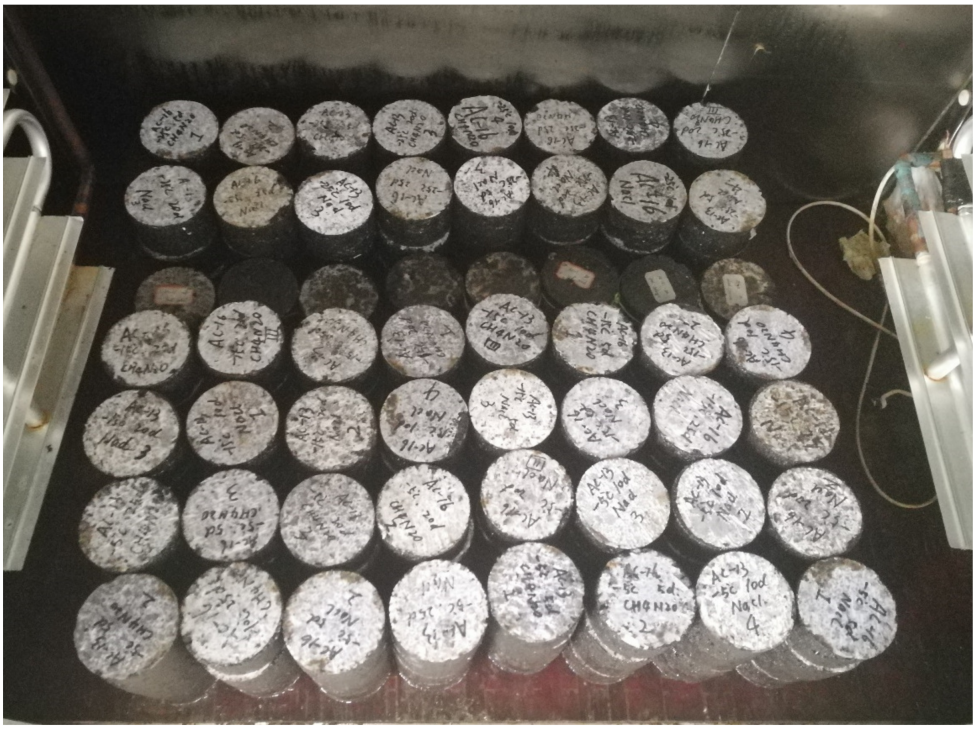


Figure 4. Test specimens frozen in the temperature control box.

3.3. Freeze–Thaw Splitting Test

Marshall specimens were fabricated per the T0702-2011 testing protocol stipulated in the "Standard Test Methods for Bitumen and Bituminous Mixtures for Highway Engineering" (JTG E20-2011) [32], maintaining a diameter of 101.6 ± 0.2 mm and a height of 63.5 ± 1.3 mm, and both sides of these specimens were compacted 50 times. Once cured, these specimens experienced freeze–thaw cycles under the influence of three varied deicer solutions and at three distinct temperatures, as per the test procedure. Following these freeze–thaw cycles, the specimens were subjected to the freeze–thaw splitting test as per the T0729-2000 testing method found in the "Standard Test Methods for Bitumen and Bituminous Mixtures for Highway Engineering" (JTG E20-2011) [32]. The specific

testing procedure involved partitioning eight Marshall specimens post freeze–thaw cycles into two sets, each containing four specimens. The second quartet of Marshall specimens underwent the following procedure: Step 1. The pressure of the vacuum drying oven was adjusted to 97.3–98.7 kPa (730–740 mmHg), and the specimens were placed inside for a duration of 15 min, following which the valve was opened to normal pressure and the specimens were subsequently submerged in water for 0.5 h. Step 2. The specimens were removed, and each of the four was placed in individual plastic bags containing approximately 10 mL of water and sealed. These bags containing the specimens were placed in a refrigerator set at a temperature of -18 ± 2 °C and subjected to low-temperature storage for 16 ± 1 h. Step 3. Subsequently, the specimens were retrieved from the refrigerator and placed in a constant temperature water bath set at 60 ± 1 °C for 24 h. Upon processing the second set of specimens, the first and second sets were collectively placed in a constant temperature water bath at 25 ± 0.5 °C for no less than 2 h. Post removal from the water bath, the specimens were immediately placed on a Marshall testing machine for the splitting test. Following the test, the tensile strength ratio was determined using Equation (2). The test was conducted using a Marshall stability tester (model SYD-0709A-1) from Shanghai Changji Geological Instrument Co., Ltd., fitted with a splitting test fixture; the loading speed was precisely controlled at 50 ± 5 mm/min.

$$TSR = \frac{\overline{R}_{T2}}{\overline{R}_{T1}} \times 100 \quad (2)$$

where:

TSR is tensile strength ratio of test specimen (%);
$\overline{R}_{T2}$ is average split tensile strength of test specimen s after freeze–thaw cycle (MPa);
$\overline{R}_{T1}$ is average split tensile strength of test specimen s without freeze–thaw cycle (MPa).

4. Analysis and Discussion of Results

4.1. Residual Stability of Asphalt Mixture after Freeze–Thaw Cycles

The outcomes from Marshall water immersion tests conducted on two distinct gradation asphalt mixtures, following freeze–thaw cycles undertaken within the three deicer solutions and three low-temperature regimes, are delineated in Figure 5.

Figure 5a illustrates that with increasing freeze–thaw cycle duration, the residual stability MS_0 across three temperatures manifests a declining trend. At −5 °C, the residual stability curve recedes slowly, recording an 11.68% reduction over the 30 cycles yet maintaining compliance with the relevant specifications throughout. However, at −15 °C and −25 °C, the residual stability curves decrease swiftly, experiencing drops of 17.07% and 18.84%, respectively, over 30 cycles, both breaching the 75% specification at the 25th and 20th cycles, respectively. Figure 5b displays a similar pattern, indicating a decreasing trend in MS_0 across the three temperatures with the progression of freeze–thaw cycles. The curve at −5 °C diminishes at a slower pace, decreasing by 13.75% over 30 cycles and failing to uphold the 75% specification at the 30th cycle. Conversely, the curves at −15 °C and −25 °C decrease rapidly, with decreases of 20.20% and 21.70%, respectively, over 30 cycles, both failing to maintain the 75% specification by the 15th cycle. As illustrated in Figure 5c, an increase in freeze–thaw cycle count correlates with a decrease in MS_0 across the three temperature conditions. The residual stability curves for −5 °C and −15 °C decrease moderately, with reductions of 3.68% and 6.70%, respectively, over 30 cycles, both maintaining compliance with the specifications throughout the cycles. On the other hand, the curve at −25 °C reduces swiftly, decreasing by 14.44% over 30 cycles and failing to uphold the 75% specification at the 30th cycle.

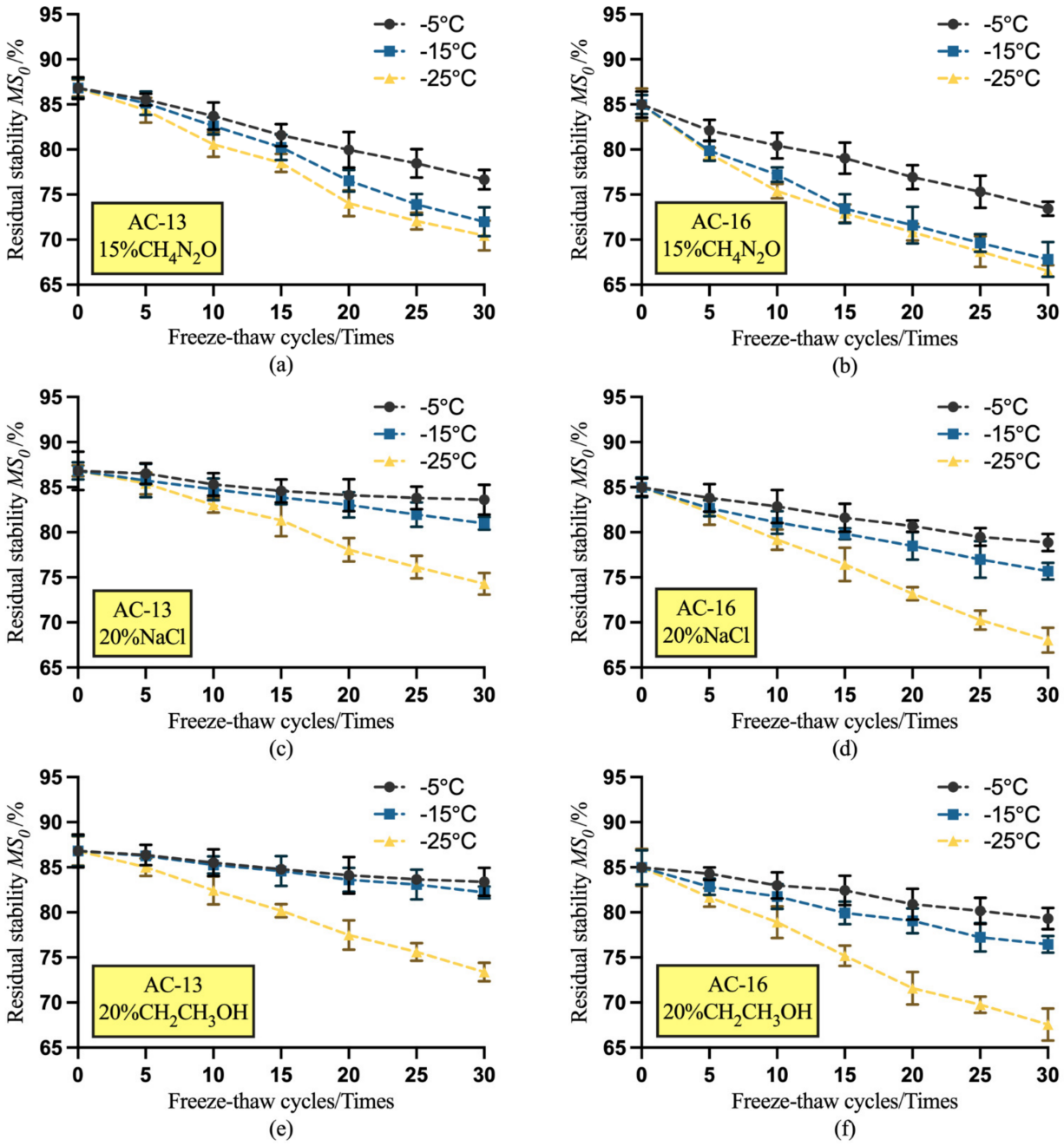


Figure 5. Changes in residual stability MS_0 with increasing freeze–thaw cycles at different temperatures: (**a**) AC-13, 15% CH_4N_2O; (**b**) AC-16, 15% CH_4N_2O; (**c**) AC-13, 20% NaCl; (**d**) AC-16, 20% NaCl; (**e**) AC-13, 20% CH_2CH_3OH; and (**f**) AC-16, 20% CH_2CH_3OH.

In Figure 5d, the accumulation of freeze–thaw cycles corresponds to a decrease in MS_0 across the three temperature conditions. The residual stability curves for −5 °C and −15°C recede moderately, with drops of 7.20% and 10.93%, respectively, over 30 cycles, both sustaining compliance with the specifications throughout. The curve at −25 °C, however, drops rapidly, decreasing by 19.92% over 30 cycles and failing to uphold the 75% specification at the 20th cycle. As depicted in Figure 5e, with an increase in freeze–thaw cycles, the MS_0 at all three temperatures continues to decline. The residual stability curves for −5 °C and −15 °C decrease slowly, with decreases of 3.96% and 5.30%, respectively, over 30 cycles, both maintaining compliance with the specifications throughout the cycles. The curve at −25 °C, however, decreases sharply by 15.48% over 30 cycles, failing to maintain the 75% specification at the 30th cycle. Finally, as shown in Figure 5f, an increase in the

count of freeze–thaw cycles coincides with a decrease in MS_0 at all temperature conditions. The residual stability curves at −5 °C and −15 °C recede moderately, with reductions of 6.66% and 10.02%, respectively, over 30 cycles, both sustaining the specifications throughout. However, the curve at −25 °C reduces drastically, recording a 20.51% decrease over 30 cycles and failing to uphold the 75% specification at the 20th cycle.

4.2. Tensile Strength Ratio of Asphalt Mixture after Freeze–Thaw Cycles

The outcomes from freeze–thaw splitting tests conducted on two distinct gradation asphalt mixtures, following freeze–thaw cycles undertaken within the three deicer solutions and three low-temperature regimes, are delineated in Figure 6.

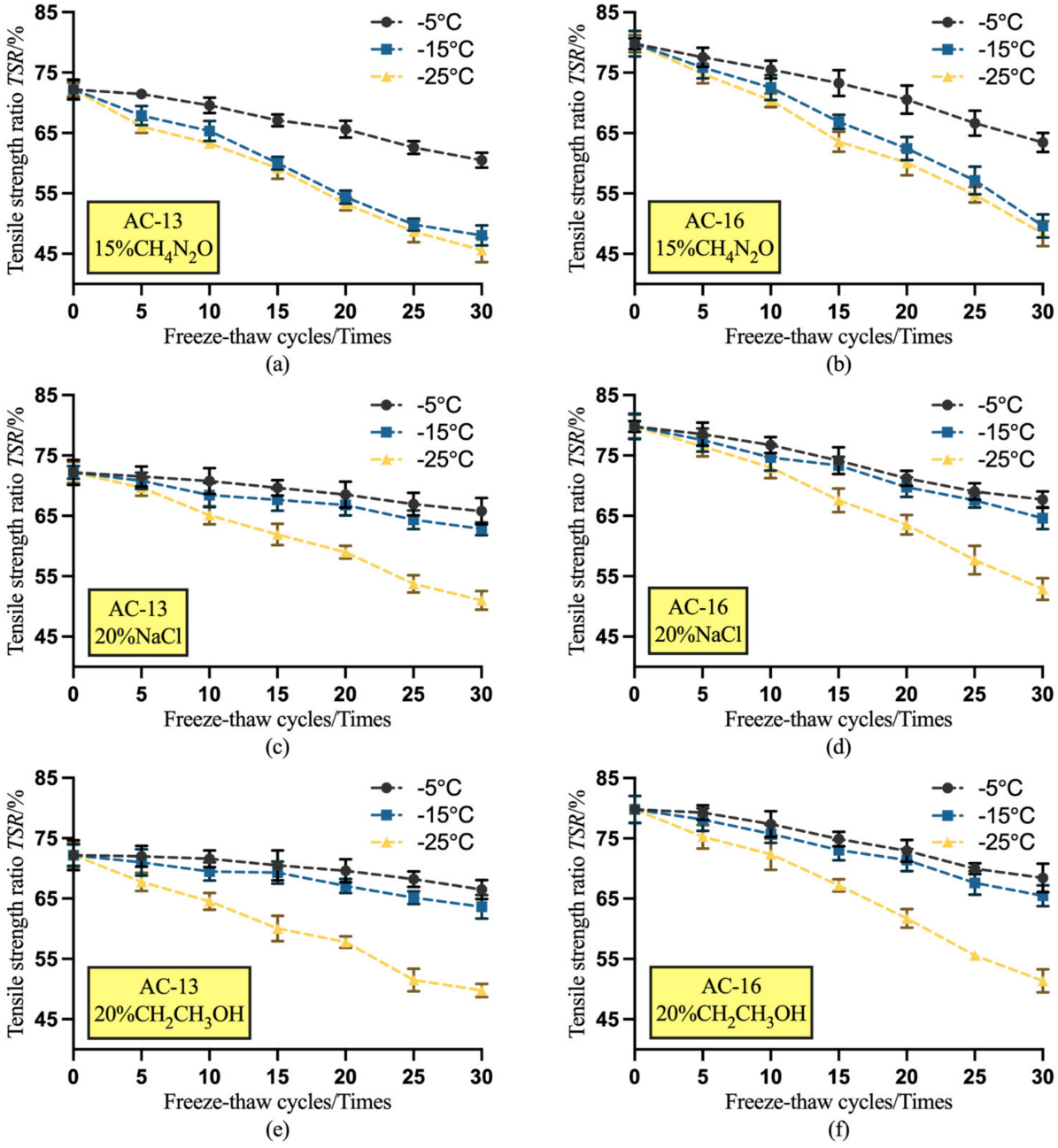


Figure 6. Changes in tensile strength ratio TSR with increasing freeze–thaw cycles at different temperatures: (**a**) AC-13, 15% CH_4N_2O; (**b**) AC-16, 15% CH_4N_2O; (**c**) AC-13, 20% NaCl; (**d**) AC-16, 20% NaCl; (**e**) AC-13, 20% CH_2CH_3OH; and (**f**) AC-16, 20% CH_2CH_3OH.

Figure 6a demonstrates that with the progression of freeze–thaw cycles, there is a downward trend in the TSR at the three specified temperatures. The TSR curve at −5 °C recedes leisurely, recording a 16.22% drop over 30 cycles, and breaches the preset minimum value of 70% at the 10th cycle. Meanwhile, the TSR curves at −15 °C and −25 °C decline swiftly, with reductions of 33.47% and 36.82%, respectively, over 30 cycles, both failing to uphold the 70% specification by the fifth cycle. As depicted in Figure 6b, the increase in freeze–thaw cycle count coincides with a decrease in TSR at all three temperature conditions. At −5 °C, the TSR curve decelerates moderately, with a drop of 20.51% over 30 cycles, and fails to sustain the 70% threshold at the 25th cycle. The TSR curves at −15 °C and −25 °C, conversely, drop markedly, decreasing by 37.85% and 39.42%, respectively, over 30 cycles, and both breach the 70% specification at the 15th cycle.

Figure 6c continues to display a similar trend, with an increase in freeze–thaw cycles resulting in a decrease in TSR at all temperatures. The TSR curves at −5 °C and −15 °C decrease at a slower pace, with reductions of 8.86% and 12.92%, respectively, over 30 cycles, falling below the 70% specification at the 15th and 10th cycles, respectively. The TSR curve at −25 °C, however, reduces drastically, falling by 29.32% over 30 cycles and failing to maintain the 70% specification at the fifth cycle. As evidenced in Figure 6d, the accumulation of freeze–thaw cycles corresponds to a decrease in TSR across the three temperature conditions. The TSR curves for −5 °C and −15 °C descend moderately, with drops of 15.17% and 19.06%, respectively, over 30 cycles, failing to uphold the 70% specification at the 25th and 20th cycles, respectively. The TSR curve at −25 °C drops drastically, decreasing by 33.76% over 30 cycles, breaching the 70% specification at the 15th cycle. Figure 6e further illustrates that with an increase in freeze–thaw cycles, the TSR across all three temperatures continues to decline. The TSR curves for −5 °C and −15 °C decrease gradually, with decreases of 7.88% and 11.84%, respectively, over 30 cycles, failing to meet the 70% specification at the 20th and 10th cycles, respectively. The TSR curve at −25 °C, on the other hand, decreases sharply by 31.07% over 30 cycles, failing to uphold the 70% specification at the fifth cycle. Finally, as shown in Figure 6f, an increase in the count of freeze–thaw cycles coincides with a decrease in TSR at all temperature conditions. The TSR curves at −5 °C and −15 °C recede moderately, with drops of 14.27% and 17.97%, respectively, over 30 cycles, both failing to uphold the 70% specification at the 25th cycle. Conversely, the TSR curve at −25 °C reduces drastically, recording a 35.61% decrease over 30 cycles, and breaches the 70% specification at the 15th cycle.

4.3. Water Stability of the Asphalt Mixture after Freeze–Thaw Cycles

As indicated in Figures 5a,b and 6a,b, at −5 °C, the 15% CH_4N_2O solution does not freeze, and this non-frozen solution safeguards the asphalt mixture from freeze-induced damage and frost heave. Notwithstanding this protection, the solution instigates a perceptible erosion to the asphalt mixture, culminating in a deterioration of residual stability by approximately 12%. Furthermore, an approximate 18% loss in TSR is observed, potentially attributed to the dissolution of certain asphalt components by the urea solution, which fosters microscopic erosion and compromises the integral stability of the material. At markedly lower temperatures of −15 °C and −25 °C, which transcend the freezing point of the 15% CH_4N_2O solution, a significant escalation in both the loss of residual stability (about 19%) and TSR deterioration (approximately 37%) is recorded. This phenomenon can be ascribed to the solution's infiltration and subsequent freezing within the voids of the asphalt mixture, consequently augmenting the void ratio. As this cycle recurs with further freeze–thaw sequences, an increased volume of solution permeates the mixture, exacerbating the specimen's degradation and precipitating a pronounced diminution in water stability.

Detailed analyses depicted in Figures 5c,d and 6c,d indicate that at temperatures of −5 °C and −15 °C, the 20% NaCl solution remains in a liquid state, thereby efficiently shielding the asphalt mixture from freezing damages. Nonetheless, the NaCl solution permeating the asphalt mixture induces erosion damage, with an observed residual stability

loss of roughly 7% and a TSR decrement of about 14%. This could be due to the formation of an unstable, water-soluble amorphous film by chloride salts on the asphalt surface, encapsulating the honeycomb structure and thereby impairing the mixture's integrity, leading to diminished water stability [35]. As the temperature plunges to −25 °C, surpassing the freezing point of the 20% NaCl solution, a pronounced decline in both residual stability (approximately 17%) and TSR (about 31%) is noted. This deterioration is attributed to the freezing of the solution that had permeated the asphalt mixture's voids, resulting in an enhanced void ratio. This phenomenon, in turn, facilitates a greater influx of the solution in subsequent freeze–thaw cycles, thereby aggravating the specimen's degradation and culminating in a substantial loss of water stability.

The data presented in Figures 5e,f and 6e,f indicate that at temperatures of −5 °C and −15 °C, the 20% CH_2CH_3OH solution remains above its freezing point, successfully shielding the asphalt mixture from freeze-related damage. Nonetheless, the introduction of the alcohol solution within the asphalt mixture still incites a level of erosive damage, culminating in an approximate 6.5% decline in residual stability and a 13% reduction in TSR. As documented in existing literature, a chemical interaction and diffusion process occurs between the alcohol and the asphalt binder, precipitating a structural degradation within the asphalt mixture, which likely contributes to the observed diminution in water stability [36]. Upon the decrease in temperature to −25 °C, which is beneath the freezing point of the 20% CH_2CH_3OH solution, a significant exacerbation in material degradation is noted, with the residual stability and TSR decreasing by about 18% and 33%, respectively. This phenomenon is attributed to the freezing of the alcohol solution once infiltrated into the asphalt mixture's voids, thereby elevating the void ratio. In successive freeze–thaw cycles, an increased quantity of solution is absorbed, amplifying the specimen's damage and resulting in a notable loss of water stability.

Per the observations from Figures 5 and 6, an increase in freeze–thaw cycles results in a more pronounced decline in residual stability and TSR for AC-16 than AC-13, regardless of whether the deicer solution reaches its freezing point. Given that the fine aggregate percentage in AC-13 surpasses that of AC-16, an increase in the percentage of fine aggregate enhances the resistance of asphalt concrete to deicer erosion and frost heave damage.

5. Significance Analysis of Influence Factor

5.1. Theoretical Basis of Analysis of Variance

Analysis of variance (ANOVA) is a statistical method that examines the influence of distinct factors on sampling data. Fundamentally, it involves computing the variance of each sample, comparing this variance with the random error variance, and discerning whether any individual factor significantly impacts the sampling data's distribution. The discrepancies in the two sets of observed data arise from both the influences of differing factors and random sampling, and these influences can be quantified using two distinct variances. The variance due to dissimilar factors is referred to as the between-groups variance, whereas the variance arising from random sampling is known as the within-groups variance. The between-groups variance encapsulates the differences instigated by both factors and sampling randomness, whereas the within-groups variance solely accounts for the differences prompted by random sampling. Consequently, the between-groups variance inherently incorporates the within-groups variance. The comparison and analysis of the influences of various factors on the observed data can be executed by computing the ratio of these two variances. If the between-groups variance to within-groups variance ratio approximates one, it signifies that the factors do not exert any influence on the sampling data, and the data discrepancies are solely due to sampling randomness. If this ratio greatly surpasses one, it implies a significant impact of the factors on the data. Conventionally, a threshold value is set, and when the ratio reaches this critical value, it can be inferred that a notable difference exists between the two variances.

5.2. Residual Stability

Variance analysis was conducted on the various influential factors and residual stability MS_0. The findings of this analysis are presented in Table 8.

Table 8. Variance analysis of various influential factors and residual stability MS_0.

Source	DF	Type III Sum of Squares	Mean Square	F	Pr > F
Number of freeze–thaw cycles	6	1689.864335	281.644056	71.96	<0.0001
Gradation	1	466.093016	466.093016	119.09	<0.0001
Temperature	2	515.676798	257.838399	65.88	<0.0001
Solution of deicer	2	317.330849	158.665424	40.54	<0.0001

Table 8 reveals that the significant difference coefficients for various influences on the asphalt mixture's residual stability are all below 0.001. This suggests that the number of freeze–thaw cycles, gradation, temperature, and deicer solution significantly affect the asphalt mixture's residual stability. The statistical F-value indicates that the gradation exerts the most substantial impact on residual stability, succeeded by the number of freeze–thaw cycles, the temperature exhibits a lesser effect, and the deicer solution has the least significance.

5.3. Tensile Strength Ratio

Variance analysis was conducted on the various influential factors and tensile strength ratio TSR. The findings of this analysis are presented in Table 9.

Table 9. Variance analysis of various influential factors and tensile strength ratio TSR.

Source	DF	Type III Sum of Squares	Mean Square	F	Pr > F
Number of freeze–thaw cycles	6	4645.354113	774.225685	74.00	<0.0001
Gradation	1	905.671598	905.671598	86.56	<0.0001
Temperature	2	1398.750941	699.375471	66.85	<0.0001
Solution of deicer	2	459.363927	229.681963	21.95	<0.0001

Table 9 demonstrates that the significant difference coefficients for various factors influencing the asphalt mixture's tensile strength ratio are uniformly below 0.001. This denotes that the number of freeze–thaw cycles, gradation, temperature, and deicer solution significantly impact the asphalt mixture's tensile strength ratio. The statistical F-value suggests that gradation yields the most potent effect on the tensile strength ratio, followed by the number of freeze–thaw cycles, the temperature influence is less pronounced, and the deicer solution presents the least substantial impact.

A comprehensive analysis of the variance results from both MS_0 and TSR reveals that the asphalt mixture gradation has the most substantial influence on both test indicators, underscoring the critical role gradation assumes in impacting the water stability of asphalt mixtures. This may be attributed to the fact that gradation directly manipulates the compactness and resilience of the mixture, hence affecting water stability [37]. Moreover, the number of freeze–thaw cycles also significantly impacts, indicating that increased freeze–thaw cycles potentially inflict more structural damage on the asphalt mixture, thereby influencing its water stability [38]. In addition, temperature exerts a significant influence, as varying temperature conditions can modify the freezing and thawing rates of water, thus impacting the degree of freeze–thaw damage. Lastly, while the deicing solution does

have an impact, primarily by altering the pore water chemical properties of the mixture, this effect is comparably minimal in relation to the other factors.

6. Conclusions

Following data analysis from the Marshall water immersion test and the freeze–thaw splitting test, which scrutinized the freeze–thaw cycles of two varieties of dense-graded asphalt mixtures subjected to three distinct deicer solutions and three unique low-temperature environments, this present study concludes as follows:

(1) Deicer solutions, once absorbed into the asphalt mixture, can shield it from frost heaving damage, provided they remain above their freezing point. The empirical data indicates a residual stability decline of approximately 8% and a TSR reduction of around 14%, suggesting a minimal loss of water stability. However, they still inflict erosion damage on the asphalt concrete, potentially shortening the lifespan of the pavement with prolonged usage.

(2) When the temperature falls beneath their freezing point after the deicer solutions penetrate the asphalt mixture, frost heaving damage to the asphalt concrete occurs, culminating in a significant water stability loss. The empirical data points to a residual stability decline of approximately 19% and a TSR reduction of about 35%, severely compromising the longevity of the road surface.

(3) Among the three deicers studied, CH_4N_2O inflicts significantly more damage on the water stability of the asphalt mixture compared to NaCl and CH_2CH_3OH.

(4) Enhancing the proportion of fine aggregate in the asphalt mixture bolsters the asphalt concrete's resistance to deicer erosion damage and frost heaving damage.

(5) Variance analysis results for the two evaluation indicators indicate that gradation significantly influences the water stability of the asphalt mixture, even more so than the deicer, without considering unmodifiable factors such as weather (distinct low-temperature environments) and pavement service time (freeze–thaw cycles). Therefore, it is advisable to modify the gradation of asphalt mixtures on icy road sections. In scenarios where gradation alteration is impossible, or the road has already been constructed, the application of deicer remains an effective means to safeguard the asphalt mixture.

The present study explores the alterations in the water stability of asphalt mixtures under varying environmental conditions, ascertained through freeze–thaw cycling tests. Such findings could offer valuable references for pavement design and maintenance, particularly in colder regions. Grasping the effects of these factors on the performance of asphalt mixtures facilitates more effective pavement design and maintenance, thereby enhancing pavement longevity and vehicular safety. Nonetheless, this research has certain constraints. Primarily, the experimental scope was limited to AC-13 and AC-16 asphalt mixtures alongside three distinct types of deicers, which may not comprehensively represent all potential asphalt mixtures and deicers. Secondly, the prevailing experimental conditions may not fully encapsulate the multifaceted scenarios encountered in real road environments. Future investigations should encompass a broader variety of asphalt mixtures and deicers and take into account additional environmental variables, such as traffic load and temperature range, to more precisely gauge the effects of these factors on asphalt mixture performance.

Author Contributions: Conceptualization, M.G. and V.P.K.; Methodology, T.N.; Software, M.G.; Formal analysis, T.N.; Investigation, T.N.; Resources, M.G.; Data curation, M.G. and T.N.; Writing—original draft, M.G. and T.N.; Writing—review & editing, M.G.; Supervision, V.P.K. and P.L.; Project administration, V.P.K. and P.L.; Funding acquisition, V.P.K. and P.L. All authors have read and agreed to the published version of the manuscript.

Funding: This work was financially supported by the China Scholarship Council (No.: 201905650001), National Natural Science Foundation of China (No.: 52368066), Lanzhou University of Technology Hongliu Outstanding Young Talent Program, China (No.: 04-062005), Natural Science Foundation of Gansu Province, China (No.: 23JRRA773), and Gansu Provincial University Innovation Fund Project (No.: 2022A-026).

Data Availability Statement: Not applicable.

Conflicts of Interest: The authors declare no conflict of interest.

References

1. Chen, Z.; Zhang, H.; Duan, H.; Shi, C. Improvement of thermal and optical responses of short-term aged thermochromic asphalt binder by warm-mix asphalt technology. *J. Clean. Prod.* **2021**, *279*, 123675. [CrossRef]
2. Ma, T.; Geng, L.; Ding, X.; Zhang, D.; Huang, X. Experimental study of deicing asphalt mixture with anti-icing additives. *Constr. Build. Mater.* **2016**, *127*, 653–662. [CrossRef]
3. Shi, X.; Veneziano, D.; Xie, N.; Gong, J. Use of chloride-based ice control products for sustainable winter maintenance: A balanced perspective. *Cold Reg. Sci. Technol.* **2013**, *86*, 104–112. [CrossRef]
4. Trenouth, W.R.; Gharabaghi, B.; Perera, N. Road salt application planning tool for winter de-icing operations. *J. Hydrol.* **2015**, *524*, 401–410. [CrossRef]
5. Hintz, W.D.; Relyea, R.A. A review of the species, community, and ecosystem impacts of road salt salinisation in fresh waters. *Freshw. Biol.* **2019**, *64*, 1081–1097. [CrossRef]
6. Coldsnow, K.D.; Mattes, B.M.; Hintz, W.D.; Relyea, R.A. Rapid evolution of tolerance to road salt in zooplankton. *Environ. Pollut.* **2017**, *222*, 367–373. [CrossRef] [PubMed]
7. Equiza, M.; Calvo-Polanco, M.; Cirelli, D.; Señorans, J.; Wartenbe, M.; Saunders, C.; Zwiazek, J. Long-term impact of road salt (NaCl) on soil and urban trees in Edmonton, Canada. *Urban For. Urban Green.* **2017**, *21*, 16–28. [CrossRef]
8. Corsi, S.R.; Geis, S.W.; Bowman, G.; Failey, G.G.; Rutter, T.D. Aquatic Toxicity of Airfield-Pavement Deicer Materials and Implications for Airport Runoff. *Environ. Sci. Technol.* **2009**, *43*, 40–46. [CrossRef]
9. Cho, S.H.; Lee, G.T.; Lee, B.D.; Kim, J.H.; Kim, D.S.; Moon, S.Y.; Lee, D.G.; Choi, J.M.; Kim, J.Y. Detected Range of the Deicer around the Highway. *Korean Soc. Road Eng.* **2018**, *05*, 120–121. Available online: https://db.koreascholar.com/Article/Detail/348286 (accessed on 12 September 2023).
10. Del Bosque, I.S.; Heede, P.V.D.; De Belie, N.; de Rojas, M.S.; Medina, C. Freeze-thaw resistance of concrete containing mixed aggregate and construction and demolition waste-additioned cement in water and de-icing salts. *Constr. Build. Mater.* **2020**, *259*, 119772. [CrossRef]
11. Khan, R.A.; Sharma, R. Strength and durability characteristics of rice husk ash concrete reinforced with polypropylene fi-bres. *Jordan J. Civ. Eng.* **2018**, *12*, 653–668.
12. Liu, J.; Zhang, W.; Li, Z.; Jin, H.; Tang, L. Influence of deicing salt on the surface properties of concrete specimens after 20 years. *Constr. Build. Mater.* **2021**, *295*, 123643. [CrossRef]
13. Qiao, C.; Suraneni, P.; Weiss, J. Damage in cement pastes exposed to NaCl solutions. *Constr. Build. Mater.* **2018**, *171*, 120–127. [CrossRef]
14. Lee, H.-J.; Kim, Y.R. Viscoelastic Continuum Damage Model of Asphalt Concrete with Healing. *J. Eng. Mech.* **1998**, *124*, 1224–1232. [CrossRef]
15. Zhang, H.; Duan, H.; Zhu, C.; Chen, Z.; Luo, H. Mini-Review on the Application of Nanomaterials in Improving Anti-Aging Properties of Asphalt. *Energy Fuels* **2021**, *35*, 11017–11036. [CrossRef]
16. Nan, T.F.; Li, P.; Mao, Y. Connections between chemical composition and rheology of aged base asphalt binders during repeated freeze-thaw cycles. *Constr. Build. Mater.* **2018**, *159*, 338–350. (In Chinese) [CrossRef]
17. Yu, H.; Ge, J.; Qian, G.; Zhang, C.; Dai, W.; Li, P. Evaluation on the rejuvenation and diffusion characteristics of waste cooking oil on aged SBS as-phalt based on molecular dynamics method. *J. Clean. Prod.* **2023**, *406*, 136998. [CrossRef]
18. Setiadji, B.H.; Utomo, S. Nahyo Effect of chemical compounds in tidal water on asphalt pavement mixture. *Int. J. Pavement Res. Technol.* **2017**, *10*, 122–130. [CrossRef]
19. Xiong, R.; Chu, C.; Qiao, N.; Wang, L.; Yang, F.; Sheng, Y.; Guan, B.; Niu, D.; Geng, J.; Chen, H. Performance evaluation of asphalt mixture exposed to dynamic water and chlorine salt erosion. *Constr. Build. Mater.* **2019**, *201*, 121–126. [CrossRef]
20. Yang, X.; Tang, H.; Cai, X.; Wu, K.; Huang, W.; Zhang, Q.; Li, H. Evaluating reclaimed asphalt mixture homogeneity using force chain transferring stress effi-ciency. *Constr. Build. Mater.* **2023**, *365*, 130050. [CrossRef]
21. Yang, L. Study on Temperature Field Prediction Model and Anti Icing Technology of Asphalt Pavement in Winter of Gansu Province. Master's Thesis, Lanzhou University of Technology, Lanzhou, China, 2018. (In Chinese)
22. Kefei, L. Study on Failure Mechanism and Remediation Technology of Asphalt Pavement under Extreme Climate. Ph.D. Thesis, Central South University, Changsha, China, 2012. (In Chinese)
23. Amini, B.; Tehrani, S.S. Simultaneous effects of salted water and water flow on asphalt concrete pavement deterioration under freeze–thaw cycles. *Int. J. Pavement Eng.* **2014**, *15*, 383–391. [CrossRef]

24. Feng, D.; Yi, J.; Wang, D.; Chen, L. Impact of salt and freeze–thaw cycles on performance of asphalt mixtures in coastal frozen region of China. *Cold Reg. Sci. Technol.* **2010**, *62*, 34–41. [CrossRef]
25. Guo, Q.; Li, G.; Gao, Y.; Wang, K.; Dong, Z.; Liu, F.; Zhu, H. Experimental investigation on bonding property of asphalt-aggregate interface under the actions of salt im-mersion and freeze-thaw cycles. *Constr. Build. Mater.* **2019**, *206*, 590–599. [CrossRef]
26. Wang, L.; Gong, N.; Xing, Y. Researching the influence factors of asphalt mixture performance under the dam-age of deicing salt and freezing-thawing cycles. *J. Funct. Mater.* **2016**, *47*, 88–93. (In Chinese)
27. Huang, X.; Sha, A.; Jiang, W.; Wang, Y. Effect and mechanism of salt erosion on performance of bitumen and asphalt mixtures. *J. Chang. Univ. Nat. Sci. Ed.* **2017**, *37*, 33–38.
28. Zhang, F.; Cao, Y.; Sha, A.; Lou, B.; Song, R.; Hu, X. Characterization of asphalt mixture using X-ray computed tomography scan technique after freeze-thaw cycle and microwave heating. *Constr. Build. Mater.* **2022**, *346*, 128435. [CrossRef]
29. Kringos, N.; Scarpas, A. Physical and mechanical moisture susceptibility of asphaltic mixtures. *Int. J. Solids Struct.* **2008**, *45*, 2671–2685. [CrossRef]
30. Wang, J.; Zhang, H.; Zhu, C. Effect of multi-scale nanocomposites on performance of asphalt binder and mixture. *Constr. Build. Mater.* **2020**, *243*, 118307. [CrossRef]
31. Li, H.; Zhang, S.; Zhao, J. Evaluation of asphalt pavement performance by matter-element theory model. *J. Munic. Technol.* **2022**, *40*, 214–219. (In Chinese)
32. Ministry of Communications of PRC. *Standard Test Methods of Bitumen and Bituminous Mixtures for Highway Engineering (JTG E20)*; China Communications Press: Beijing, China, 2011. (In Chinese)
33. Ministry of Communications of PRC. *Technical Specification for Construction of Highway Asphalt Pavements (JTG F40)*; China Communications Press: Beijing, China, 2017. (In Chinese)
34. Ministry of Communications of PRC. *Test Methods of Aggregate for Highway Engineering (JTG E42)*; China Communications Press: Beijing, China, 2017. (In Chinese)
35. Long, Z.; Guo, N.; Tang, X.; Ding, Y.; You, L.; Xu, F. Microstructural evolution of asphalt induced by chloride salt erosion. *Constr. Build. Mater.* **2022**, *343*, 128056. [CrossRef]
36. Falchetto, A.C.; Turos, M.I.; Marasteanu, M.O. Investigation on asphalt binder strength at low temperatures. *Road Mater. Pavement Des.* **2012**, *13*, 804–816. [CrossRef]
37. Liu, S.; Zhu, L.; Zhang, H.; Liu, T.; Ji, P.; Cao, W. Effect of Gradation Variability on Volume Parameter and Key Performances of HMA. *Front. Mater.* **2021**, *7*, 611409. [CrossRef]
38. Din, I.M.U.; Mir, M.S.; Farooq, M.A. Effect of freeze-thaw cycles on the properties of asphalt pavements in cold regions: A review. *Transp. Res. Procedia* **2020**, *48*, 3634–3641. [CrossRef]

Disclaimer/Publisher's Note: The statements, opinions and data contained in all publications are solely those of the individual author(s) and contributor(s) and not of MDPI and/or the editor(s). MDPI and/or the editor(s) disclaim responsibility for any injury to people or property resulting from any ideas, methods, instructions or products referred to in the content.